Three-dimensional finite element analysis of multi-stage hot forming of railway wheels. Int J Adv Manuf Technol

ARTICLE *in* INTERNATIONAL JOURNAL OF ADVANCED MANUFACTURING TECHNOLOGY · MARCH 2011

Impact Factor: 1.46 · DOI: 10.1007/s00170-010-2810-4

4 AUTHORS, INCLUDING:

R.K. Ohdar
National Institute of Foundry & Forge Tech…
30 PUBLICATIONS **298** CITATIONS
SEE PROFILE

Dilip Kumar Pratihar
IIT Kharagpur
169 PUBLICATIONS **1,187** CITATIONS
SEE PROFILE

Indrajit Basak
National Institute of Technology, Durgapur
9 PUBLICATIONS **131** CITATIONS
SEE PROFILE

Int J Adv Manuf Technol (2011) 53:301–312
DOI 10.1007/s00170-010-2810-4

ORIGINAL ARTICLE

Three-dimensional finite element analysis of multi-stage hot forming of railway wheels

Tapas Gangopadhyay · Raj Kumar Ohdar · Dilip Kumar Pratihar · Indrajit Basak

Received: 11 February 2010 / Accepted: 21 June 2010 / Published online: 9 July 2010

Abstract Three-dimensional finite element analyses has been carried out using DEFORM 3D software on multi-stage hot forming of railway wheels involving the processes of upsetting, forging, and punching of wheels. Thermal analysis related to heating the blank in furnace and all intermediate heat transfer stages between deforming operations have been conducted. Rigid viscoplastic finite element method has been utilized for coupled thermo-mechanical analysis of the processes. Modeling of punching the wheel bore has been carried out using *Cockcroft and Latham* fracture criterion. Evolution of thermo-mechanical parameters at selected points within the workpiece has been studied in detail. The method of simulating the effects of various process parameters has been explained using relevant mathematical relations. This study shows that design, optimization, and analysis of process perturbations for multi-stage railway wheel manufacturing process can be done efficiently in three-dimensional finite element simulations instead of conventional time and cost intensive trials. It might be necessary to use the results of finite element analysis in shop-floor to enhance productivity and reduce wheel rejection.

Keywords Multi-stage hot forging · Upsetting · Piercing · Finite element analysis

T. Gangopadhyay
Central Mechanical Engineering Research Institute,
Durgapur 713209, India

R. K. Ohdar
National Institute of Foundry & Forge Technology,
Hatia,
Ranchi 834003, India

D. K. Pratihar (✉)
Department of Mechanical Engineering,
Indian Institute of Technology,
Kharagpur 721302, India
e-mail: dkpra@mech.iitkgp.ernet.in

I. Basak
Department of Mechanical Engineering,
National Institute of Technology,
Durgapur 713209, India

1 Introduction

Multi-stage hot forging process is considered as one of the most economical methods of manufacturing railway wheels (refer to Fig. 1). A typical method [1, 2] involves heating the blank in a furnace for about 6–8 h in three stages, which are, preheating at 950°C, then heating at 1,175°C, and finally soaking at 1,280°C (refer to Fig. 2). It is then transferred to the upsetting lower die and let to stand for a few seconds where some die chilling occurs. The cylindrical blank is then upset to a disk-shaped preform (refer to Fig. 4) in a hydraulic press suit. It is then moved to the forging lower die by a manipulator. Here too, heat loss to the environment and die chilling occurs. The wheels are then forged to the desired shape (refer to Fig. 10) and size. After being transferred to the punching lower die, the wheel bore is punched. The wheel is then reheated in the furnace to around 1,200°C, and the ring rolling operation is carried out. The rolled wheels are pressed further to give a dish-like shape in an operation called dishing, to cope with the bending load due to side thrust. Finally, the wheels are machined to the required size.

A large number of parameters control the quality of the wheel in multi-stage hot forming process. Among them, die geometry, flow stress, and interface friction determine the material's movement inside the die, which ultimately

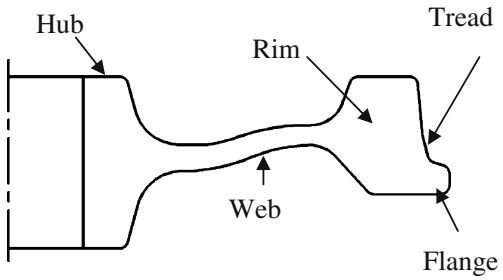

Fig. 1 Sectional profile of a railway wheel with nomenclature [1]

determines lap formation, under-filling of die cavity, die wear etc. The maximum press load depends on the flow stress, which is again dependent on temperature and strain rate. It depends on interface friction too. Die chilling reduces the temperature at workpiece surface, which increases the possibility of surface crack development. Dynamic recrystallization of material between two deformation stages influences the microstructure of the formed wheel. Process conditions like environmental temperature variation, change in coolant flows in dies, variations in transfer times, initial die temperature, die mismatch, draft angles of cast ingots used for the preparation of blank, eccentricity due to off-center placement of blank on upsetting die, inclined seating of blank on upsetting die due to the defective saw cut, etc., also affect wheel production. Other than workpiece temperature, the clearance between punch and die, punch and die radius, etc., play important role in the punching of wheel bore.

The quality of the wheel produced and its rate of rejection depend on the selection of process parameters, which is difficult because of the highly complex interrelationships among them. Moreover, a rapid change has come in railway wheel manufacturing technology and there is a need for high-speed wheels. Demands for the wheels of various shapes, sizes, and quality produced in smaller batches with short lead time [2] have been felt, recently. This requires frequent changes in production set-up and puts a challenge to the manufacturing companies for meeting the target quantity and quality. Under these circumstances, enhancing the understanding of multi-stage hot forming processes is the only way to increase wheel production by reducing the rejections. Traditional trial and error method of studying the processes encompasses theoretical and practical aspects of wheel manufacturing, and is very time-consuming, costly, and needs interruption of the actual production. A low-cost off-line method for carrying out the same study is through numerical simulations using finite element (FE) analysis. In this context, it may be mentioned that axi-symmetric simulation cannot identify the occurrence of errors due to process perturbations like eccentricity, die mismatch, defective saw cut, etc., at the early stages of wheel forming and their progression through the subsequent processes like ring rolling and dishing. Hence, the need for three-dimensional (3D) finite element analyses for the hot working processes has been felt. It is generally believed that the sources of errors in the multi-stage wheel forming process are in the initial three hot forming operations and ring rolling is the corrective process [2]. Ring growth of wheel rim portion can be predicted only by a 3D FE analysis and simulation of punching in 3D is the prerequisite. So, the decision has been taken to study the first three processes in 3D FE analysis.

An attempt has been made in the present work, to analyze the upsetting, forging, and punching processes of railway wheel manufacturing in three dimensions, which has not been reported till date to the best of the authors' knowledge. To understand the preform shape, material flow inside the dies, under-filling of die cavity, formation and propagation of folding errors through the processes, evolution of temperature, stresses, occurrence of die chilling, press load and effect of using excess material, etc., FE analysis has been carried out using DEFORM-3D software.

2 Literature review

Several attempts had been made in the past to analyze multi-stage hot-forged products by various investigators. Survey also reveals that only two papers [2, 6] reported simulation of railway wheel forging process. In the literature survey, emphasis has been given to those studies (as discussed below), which analyze phenomena similar to that occur in multi-stage wheel forging.

Minimization of forging load and control over die wear in wheel forging can be achieved by designing a good

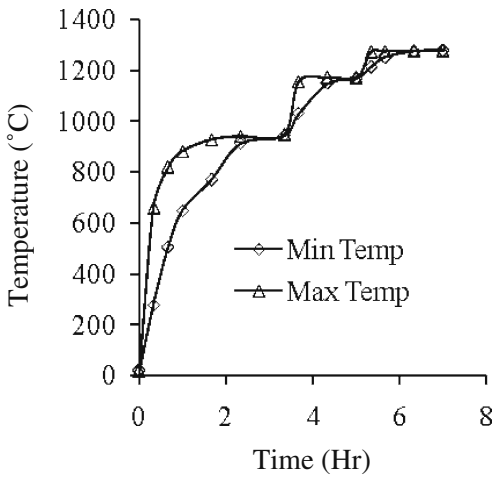

Fig. 2 Temperature difference inside the 485 kg blank during three stages of furnace heating: preheating (at 950°C); heating (at 1,175°C), and soaking (at 1,280°C)

perform, which ensures minimum metal flow inside the finished die and just fills it. In case of a monoblock wheel, preform is made from a cylindrical blank in the upsetting process. Ward et al. [2] simulated railway wheel and tire forming processes in two dimensions for ABB Diamler-Benz Transportation Company, Manchester, UK, in FE software called DEFORM-2D. The objective of their work was to find an alternative preform for which overall product quality would improve. A closed-die two-stage hot forging process was analyzed by Kim et al. [3] using 2D thermo-viscoplastic FE method with the objective of getting information on material flow, die pressure, and blank temperature. Optimization of a two-stage hot forging process was carried out by António et al. [4] using FE along with a Genetic Algorithm (GA). An objective function was designed for minimizing both the process energy as well as distance between the FE-predicted workpiece shape and the required shape subjected to a maximum value of work temperature. Lv et al. [5] simulated the four-stage forging process of a gas turbine compressor blade using 3D rigid-viscoplastic FE method. It consisted of upsetting, heading, busting, and final forging stages.

Davey et al. [6] investigated for the right strategies for axisymmetric modeling of railway wheel forming processes, so that the results could be utilized effectively. Early failure of die and under-filling of cavity for a three-stage gear blank forging operation had been analyzed by Santos et al. [7] in 2D FE software. Change in forging sequence for proper filling without excess upset and additional cooling of dies were suggested as the remedies. The effectiveness of 3D FE simulation in forging using QForm software was tested by Biba et al. [8]. The formation of a lap due to circumferential material flow for a non-symmetric cup forging had been described in their work using surface-to-surface contact. Optimum die design for a forged part with a flat thin flange using simulation results was also presented. Isothermal analysis of a titanium alloy aerofoil blade was carried out by Hu et al. [9] using 3D FE modeling. Localized plastic deformation of die surfaces at the end of the process due to very high contact pressure was predicted in their work. Wan-peng et al. [10] investigated the isothermal forging of 4A11 aluminum alloy piston skirt used in IC engines in 3D FE method. Effects of temperature, friction factor, etc., on deformation pattern, influence of punch velocity on forging load, and metal flow were analyzed.

Punching of hole in metal is usually simulated using damage criteria for ductile fracture of the metal. Cockcroft et al. [11] proposed true ductility of a metal and described a condition for damage known as Cockcroft and Latham criterion. Ko et al. [12] described a method to predict the wear of piercing tool. The effectiveness of the scheme was verified by carrying out wear analysis of piercing punch of a multi-stage forming of piston pin. Cetinkaya [13] studied the clearance between punch and die during piercing of sheet metal using an FE method. An analysis was carried out on the formation of multiple cracks on phosphor bronze metal strip using ANSYS/LS-DYNA software. Burrs formed during piercing were considered as the potential reason for defects in tire rolling and were analyzed by Ward et al. [2]. The problem was eliminated by finding a proper bore angle.

An overview of FE simulations on hot forging process and associated topics was presented by Hartley et al. [14]. According to them, more emphasis should be given on application of simulations rather than the mathematical formulations. The paper also mentioned that the forging process including the influences of involved equipment in the process had to be simulated as a whole for the interest of using FE simulation in industry.

The above literature review shows that 3D coupled thermo-mechanical FE analysis of multi-stage hot forging process could provide the insight of the process for actual production environment. Important equipment selection criteria like press load; die cooling requirement, etc., for each stage can also be established. It is clear that practical issues of railway wheel forging like eccentricity, irregularities in blank preparation, die mismatch, etc., cannot be analyzed using 2D axisymmetric FE model. It can be done in 3D only, but no such attempt has yet been made. Punching has to be modeled in 3D, so that the distribution of thermo-mechanical parameters at the end of the process can be used as the input for 3D ring rolling of wheel. Though designers may use 2D simulation results for wheel manufacturing process design and optimization, it is difficult for the shop-floor people to correlate between 2D results and the problems arising in actual production. It is understood that 3D FE analysis will give an in-depth knowledge of these processes and will help immensely in meeting the rapid changes of products, and thereby, reducing manufacturing cost and increasing profit.

The remaining part of the manuscript has been organized as follows: Section 3 presents mathematical formulations of the problems. Results of 3D FE analysis related to upsetting, forging and punching processes along with necessary heat transfer stages have been presented, discussed, and compared with those available in the published literatures in Section 4. Conclusions of the presented study have been drawn in Section 5. The scope of future work has been discussed in Section 6.

3 Mathematical formulations

In the analysis of hot forging, the flow of material through dies is of primary interest, so the flow formulation of FE

analysis [15] has been used. The time-dependent behavior of material is described by rigid-viscoplasticity and the relation between stress and strain rate is established using constitutive equation similar to that of Levy–Mises as given below.

$$\dot{\varepsilon}_{ij} = \frac{3}{2}\frac{\dot{\bar{\varepsilon}}}{\bar{\sigma}}\sigma_{ij'}, \tag{1}$$

where $\dot{\bar{\varepsilon}} = \sqrt{(2/3)}\left\{\dot{\varepsilon}_{ij}\dot{\varepsilon}_{ij}\right\}^{1/2}$ is the effective strain rate, $\bar{\sigma} = \sqrt{3/2}\left\{\sigma_{ij'}\sigma_{ij'}\right\}^{1/2}$ is the effective stress or flow stress, $\sigma_{ij'}$ *and* $\dot{\varepsilon}_{ij}$ are the components of deviatoric stress tensor and components of strain rate tensor, respectively.

Press load and various stresses in forging process depend mainly on flow stress of the deforming material, part geometry, and die-blank interface friction condition. Other than chemical composition and microstructure of workpiece material, the flow stress grossly depends on the thermo-mechanical process parameters, namely temperature (T), strain $(\bar{\varepsilon})$ and strain rate. Mathematically, it is represented as follows:

$$\bar{\sigma} = f\left(T, \bar{\varepsilon}, \dot{\bar{\varepsilon}}\right) \tag{2}$$

According to the variational approach for rigid-viscoplastic FE formulation, the solution (u_i) to a problem should give a stationary value to the following functional

$$\pi = \int_V E\left(\dot{\varepsilon}_{ij}\right)dV - \int_{S_F} F_i u_i dS, \tag{3}$$

where $E\left(\dot{\varepsilon}_{ij}\right)$ and F_i are the work function and surface tractions, respectively, over the surface S_F. The constraint for material incompressibility on admissible velocity fields is removed using a large positive penalty constant K as

$$\delta\pi = \int_V \bar{\sigma}\delta\dot{\bar{\varepsilon}}dV + K\int_V \dot{\varepsilon}_v\delta\dot{\varepsilon}_v dV - \int_{S_F} F_i\delta u_i dS = 0, \tag{4}$$

where the first integral defines the plastic work; the second one maintains volume constancy by multiplying penalty constant to the change in volume and the last integral expresses the surface traction work. Here, $\dot{\varepsilon}_v$ represents the volumetric strain rate. The solution to the above equation for complex geometrical shape is obtained by FE analysis, where the whole domain is discretized into a finite number of small regions called elements. The elemental equations are set and assembled to a global stiffness equation as follows:

$$\mathrm{K}\,\Delta\mathrm{v} = f\,, \tag{5}$$

where K is the global stiffness matrix, Δv is the incremental velocity, and f is the global force vector.

In forging, heat is generated due to plastic work and interface friction. As a result, blank temperature rises. Heat is conducted to the dies from the blank at the same time. Again, heat loss occurs due to convection and radiation to the environment at the free surface. This results in a temperature gradient within the blank and the flow stress varies considerably. These effects are taken into account by carrying out coupled thermo-viscoplastic analysis. It starts from the energy balance equation as given below:

$$k_1 T_{,ii} + \dot{r} - \rho c\dot{T} = 0, \tag{6}$$

where k_1 is the thermal conductivity, $T_{,ii}$ represents the Laplace differential operator on temperature, $k_1 T_{,ii}$ is the heat transfer rate, $\dot{r}$ is the heat generation rate, $\dot{T}$ is the time derivative of temperature and $\rho c\dot{T}$ is the internal energy rate. Heat generation in the workpiece can be determined using the following equation:

$$\dot{r} = \kappa\sigma_{ij}\dot{\varepsilon}_{ij}, \tag{7}$$

where κ represents the fraction of mechanical work that gets transformed into heat during deformation.

Friction between tool and workpiece plays an important role in metal forging process. It produces a shear force at the interface that restricts movement of metal in die. The magnitude of the developed shear frictional stress at the interface influences the deformation pattern, temperature rise, tool deflection, total force requirement during forming, etc; and is expressed as follows:

$$f_s = mkl \cong \left\{\frac{2}{\pi}\tan^{-1}\left(\frac{|u_s|}{u_0}\right)\right\}l, \tag{8}$$

where f_s and l are the frictional stress and unit vector opposite to relative sliding, respectively, u_s represents the relative sliding velocity of material, and u_0 is a small positive number.

Again, the energy balance equation can be written using FE formulation as follows:

$$C\dot{T} + K_c T = Q, \tag{9}$$

where C and K_c are the heat capacity matrix and heat conduction matrix, respectively. T and $\dot{T}$ denote the nodal temperature vector and nodal temperature rate vectors, respectively. The heat flux vector is denoted by Q. In coupled FE analysis, the deformation Eq. 5 for a given temperature distribution and heat transfer Eq. 9 are solved simultaneously.

A small time increment (Δt) is used to maintain solution stability and is calculated using the equation given below:

$$\Delta t \le \min\left(L^{el}\sqrt{\frac{\rho}{\lambda + 2\mu}}\right), \tag{10}$$

where L^{el} is the characteristic length of an element, ρ is the density of the material, and symbols λ and μ are the effective Lamé's constants.

Effective stress indicates the onset of plastic deformation in metal and is expressed by the equation:

$$\overline{\sigma} = \left\{ \frac{(\sigma_1 - \sigma_2)^2 + (\sigma_2 - \sigma_3)^2 + (\sigma_3 - \sigma_1)^2}{2} \right\}^{1/2}, \quad (11)$$

where σ_1, σ_2, and σ_3 are the three principal stresses.

Punching has been simulated using normalized *Cockcroft and Latham* criterion-based damage softening method [11]. When the cumulative damage C in an element reaches a critical value, according to the criterion, fracture occurs in a ductile material and is given by

$$C = \int_0^{\varepsilon_f} \left(\frac{\sigma^*}{\overline{\sigma}} \right) d\overline{\varepsilon}, \quad (12)$$

where $\overline{\sigma}$ is the equivalent stress, ε_f is the fracture strain, σ^* is the peak tensile stress and $\overline{\varepsilon}$ is the equivalent strain. The flow stress of an element reduces to a lower value, when C reaches the critical value. The value of damage criterion of a material under hydrostatic pressure gets reduced and it is found in the literature as follows:

$$C = \int_0^{\varepsilon_f} \left(\sigma^* - P \right) d\overline{\varepsilon}, \quad (13)$$

where P is the superimposed hydrostatic pressure used during tensile test of material.

4 Results and discussion

A 485-kg cylindrical blank of Ø358.4mm×615mm has been used for the simulation. Due to the similarity in composition with wheel material [1], AISI 1045 steel has been used. Tabulated flow stress data at 899°C, 999°C, 1,099°C, and 1,199°C temperatures and at 0.1/s, 100/s strain rates have been used from DEFORM 3D database. The fraction of mechanical work that gets transformed into heat has been taken as 0.95 [2] for the simulation. To reduce the simulation time, only $\frac{1}{12}$th model of the blank and dies has been used throughout the analysis. Eighteen thousand four hundred twenty-eight 3D tetrahedral elements have been used for the simulation at the beginning. Lagrangian incremental method along with a global remeshing strategy has been implemented. The maximum allowable time increment was 1.5 s. Temperature-dependent thermal conductivity and heat capacity for a range of 100°C–1,485°C have been used from DEFORM 3D database. Constant emissivity of 0.7 and convection coefficient of 0.02 N/s/mm/°C have been used for free surfaces of the workpiece.

The blank heating in furnace has been simulated in three stages. Variations of minimum and maximum temperatures for each stage of furnace heating have been recorded (refer to Fig. 2). During preheating of blank, temperature stabilizes at 950°C in 3.75 h, that at 1,175°C in 5.4 h during heating and that at 1,280°C in 7.30 h during soaking.

Insufficient blank heating causes lower core temperature, which results in higher flow stress in the core. This leads to non-uniform material flow during upsetting and material may get sucked into the body from the surface layers resulting in a flow-through defect. The non-isothermal simulation has captured the temperature-changing phenomena perfectly. The predicted required time to reach the homogeneous temperature in the blank is in good agreement with that in practice [1]. Direct measurement of core temperature is not possible physically, and thermal simulation results can be used in industry to establish the required heating time effectively.

The transfer of blank from furnace to the lower upsetting die has been simulated in 15 s for an environmental temperature of 20°C. During the transfer of blank from the furnace to the lower upsetting die, heat transfer takes place with the ambient. The minimum temperature at surface reduces to 1,075°C at the end of the process (refer to Fig. 3), while the temperature at the core remains almost unchanged, which agrees with natural phenomena.

The result indicates rapid fall in surface temperature with time. It is expected that with lower ambient temperature during winter, there will be more rapid fall in surface temperature. This along with die chilling may lead to the development of surface cracks during upsetting. Simulation may be carried out with various possible ambient temperatures to determine the maximum allowable transfer time for industrial use.

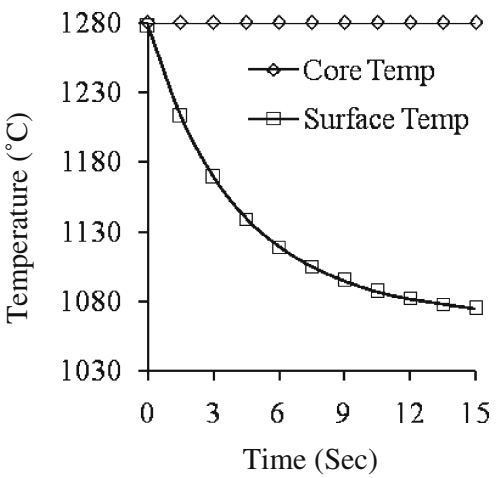

Fig. 3 Cooling of 485 kg blank during transfer from heating furnace to the lower upsetting die

Chilling of blank on lower upsetting die has been simulated using a dwell of 10 s. Dies are modeled as rigid objects having 33,076 and 33,012 elements for top and bottom dies, respectively. AISI H13 steel has been assigned as the material for dies of all stages and initial temperature of dies has been set at 20°C [2]. An interface heat transfer coefficient of 1 N/s/mm/°C has been utilized. Die chilling simulation shows that a considerable amount of heat transfer takes place during the period. Temperature of the blank surface in touch with the bottom die at the end of simulation has been recorded to be as low as 906°C. It has been observed that temperature gradient is prominent up to a few millimeters inside the blank surface, and most of the core area remains at 1,279.4°C. The temperature of the bottom die surface in contact with the hot blank reaches as high as 361°C.

Result shows that significant heat loss occurs in die chilling, and the flow stress increases at the contact surface. Excessive die chilling may lead to the development of surface defects though the temperature rise at die surface has the positive effect of developing less compressive surface stress at peak press load [2]. Simulation may be carried out to find maximum allowable die chilling time, which may further be used to determine table speed of press suit.

4.1 Upsetting of blank

Simulation of upsetting has been by carried out by bringing the upper die in contact with the blank. During simulation, it moves 490 mm to reduce the blank height to 125 mm (refer to Fig. 4). Speed of the die has been set to 43.36 mm/s. Press power limit has been described by a force-speed function for top die movement [2]. Constant time increment of 0.5 s has been used for the simulation and volume compensation has been activated. At the blank–die interface, a heat transfer coefficient of 11 N/s/mm/°C has been utilized. Self-contact has been defined to capture folding and to represent interface condition; a value of m equal to 0.7 has been used in the present work, as utilized in [9].

Deformed mesh (refer to Fig. 4) at the end of upsetting is in good agreement with the shape of the preform [1] and

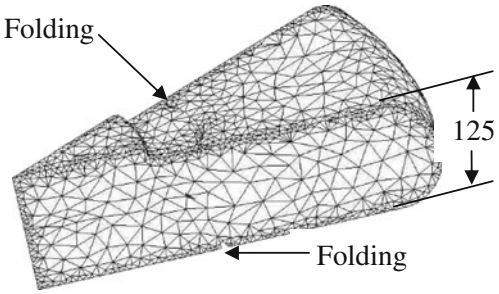

Fig. 4 FE mesh of 485 kg blank at the end of upsetting

shows that folding occurs on its upper and lower surfaces. The maximum temperature at the core of the workpiece is found to be equal to 1,308°C. Simulation also predicts a minimum temperature of 622°C at the surface of the preform. The evolution of temperature inside the blank has been studied by taking points at seven radius ratios (*RR*) ranging from $\frac{r}{8}$ to $\frac{7r}{8}$, where r stands for the maximum radius of a node from blank axis in a simulation step (refer to Fig. 5). The value of axial coordinate of the points has been taken at the middle of the final preform height. It has been observed that up to a $RR = \frac{6r}{8}$, the temperature of the blank remains almost unchanged and increases slightly at the end of the stroke. Temperature varies only at *RR* equal to $\frac{7r}{8}$ and reaches the minimum at around 140 mm of stroke. The temperatures of top and bottom dies at the end of simulation have been found to be equal to 834°C and 681°C, respectively. Results of FE simulation also show that there are some changes in the values of the effective stress (refer to Fig. 6) up to $RR = \frac{6r}{8}$, but it remains within 28 MPa. For a range of 100 mm-300 mm die stroke and at $RR = \frac{7r}{8}$, that is, near the outer surface of the preform, its value increases to as high as 48 MPa. Grid lines at seven *RR* values (refer to Fig. 7) indicate a very good radial metal flow during the upsetting operation. Distributions of axial compressive stress (refer to Fig. 8) at various *RRs* have been studied. It decreases with the increase in *RR*. Axial stress increases with the die stroke and as a result, the press load also increases with it (refer to Fig. 9). The FE simulation has predicted a press load of 3.2MN for $\frac{1}{12}$ of blank upsetting.

The maximum temperature of the workpiece is outside the forging window of AISI 1045 steel. Similar phenomenon of rise in core temperature during bulk forging of a turbine blade has been has been reported in literature [9]. A high core temperature at the time of upsetting does not affect wheel quality due to subsequent re-heating for further forming operations to produce the final shape and size. The small variation of temperatures inside the preform indicates that throughout the upsetting process, the flow stress or effective stress does not change much in the majority portion except near the surface. This indicates that material deformation is homogeneous. Increase in effective stress at $RR = \frac{7r}{8}$ is due to the low temperature at that region. Achieving right flow pattern in the preform helps in controlling the errors like flow line outcrops during further deformation in the forging stage. Simulation also shows the formation and growth of folding defect on preform surface. The information may be utilized while designing dies in industry. Perfect material distribution pattern obtained in the preform is due to the large blank height to diameter ratio [16]. Therefore, in industry, the ideal ratio of a blank for a particular wheel preform may be determined by studying the FE simulated material distribution pattern. Literature

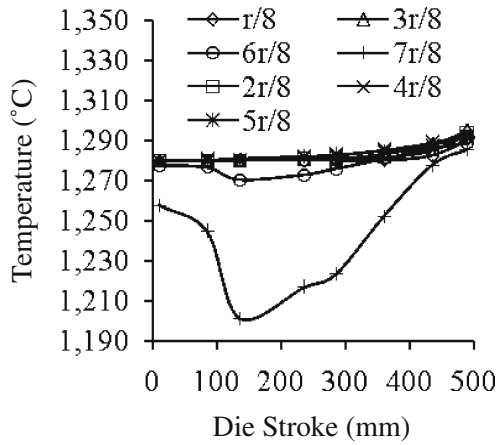

Fig. 5 Temperature at different radius ratios inside the 485 kg blank during upsetting to a 125-mm thick preform

survey reveals that the axial stress for forging a disk-like part increases from the flash gap to the center [17]. Obtained stress distribution for various *RR* corroborates it.

4.2 Forging of wheel

Preform gets transferred to forging bottom die by an automatic manipulator in about 15 s. During this period, it loses heat to the environment, and flow stress changes accordingly. Simulation of this heat transfer has been carried out to get the temperature profile of the workpiece. The maximum and minimum temperatures recorded at the end of the transfer of preform to the forging bottom die have been found to be equal to 1,300.7°C and 923°C, respectively. It is quite obvious that heat flows from the core to the surface and the temperature gradient reduces. As a result, flow stress in the preform becomes uniform.

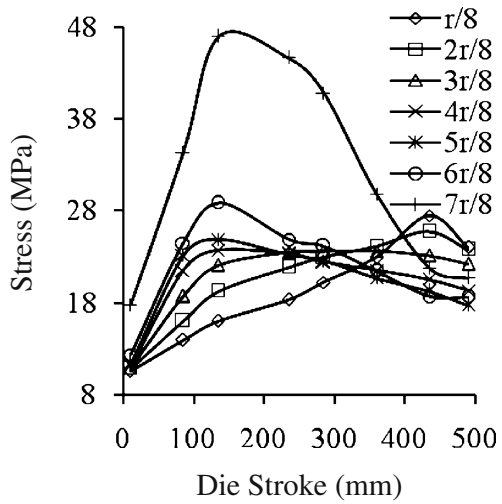

Fig. 6 Magnitude of effective stress at different radius ratios inside the 485 kg blank during upsetting to a 125 mm thick preform

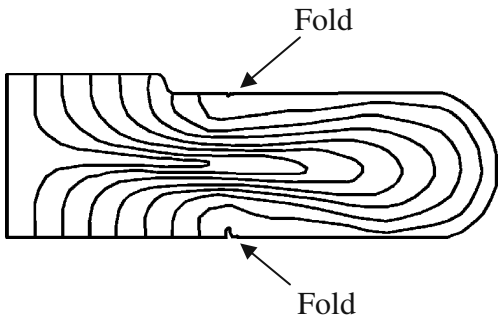

Fig. 7 Material flow shown by seven grid lines constructed at radius ratios from r/8 to 7r/8 at the end of upsetting 485 kg blank to a 125-mm thick preform

Number of elements generated for top and bottom forging dies are 43,645 and 48,015, respectively. Dynamic recrystallization of workpiece material starts after each strain interval [18] and has been simulated by initializing the distribution of effective stress in the workpiece before a forming operation [2]. Chilling of preform on forging lower die has been simulated for 7 s using a convection coefficient of 1 N/s/mm/°C. Initial temperatures of dies and environment for the simulation have been taken as 20°C. The maximum and minimum temperatures found at the end of die chilling are1290°C and 800°C, respectively. The bottom die temperature near the zone in contact with preform increases to 290°C. A possible reason for comparatively less temperature rise in forging die during free-resting than that in upsetting lower die is the relatively less area of contact.

Upper die deforms the workpiece from 125 mm preform thickness to a forged wheel of 42-mm web thickness. Speed of the die has been set to 14.31 mm/s. Time increment and heat transfer coefficient at the blank–die interface have been set to 0.5 s and 11 N/s/mm/°C, respectively, for the simulation. The final mesh at the end of forging (refer to

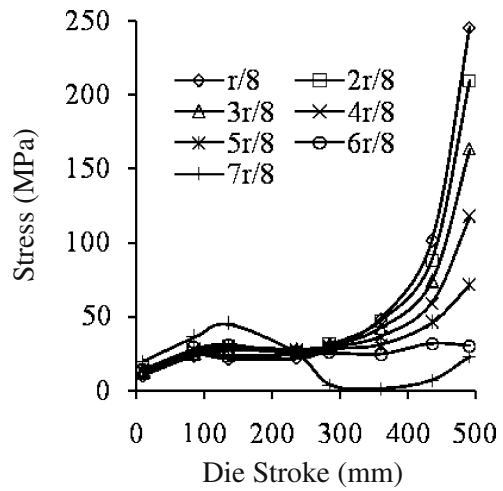

Fig. 8 Axial compressive stress at different radius ratios for 485 kg blank during upsetting to a 125 mm thick preform

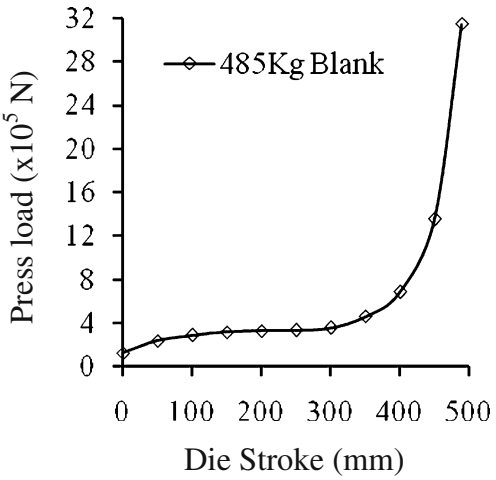

Fig. 9 FE-predicted press load for upsetting 485 kg blank to a 125 mm thick preform

Fig. 10) is in good agreement with the shape of the forged wheel [1, 6] and shows that the folding which had occurred during the upsetting stage, still exists and has been propagated towards the wheel rim. The flow of material within the die cavity during forging has been traced using axial grid lines at seven *RRs* (refer to Fig. 11) ranging from $\frac{r}{8}$ to $\frac{7r}{8}$. Location of the neutral region has been found in the middle of wheel web. Evolution of temperature inside the forged wheel has been tracked by defining seven points as done earlier (refer to Fig. 12). Axial coordinate of the points has been taken at the middle of the forged wheel web. Material near the points defined at $RR = \frac{r}{8}$ and $RR = \frac{2r}{8}$ remains within the hub cavity and initially, there is a sharp rise in temperature at those regions due to plastic work. With an increase in die stroke, cavity gets filled up, material comes into contact of dies under a high pressure, and rapid heat transfer takes place at the interface. As a result, temperature at those regions stabilizes. Near the point defined at $RR = \frac{3r}{8}$, temperature rises at a steady rate from the beginning of die stroke due to the difference between heat generation and interface heat loss. The material undergoes a very high deformation near the points defined

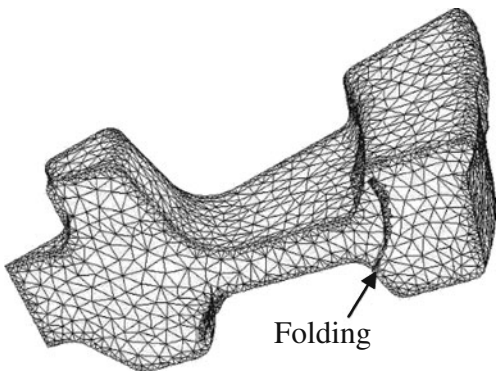

Fig. 10 FE mesh of 485 kg blank at the end of forging

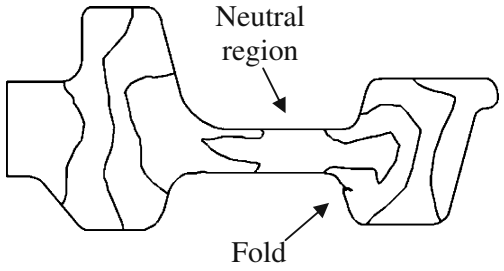

Fig. 11 Material flow shown by seven grid lines constructed at radius ratios from r/8 to 7r/8 at the end of forging of 485 kg blank from a 125-mm thick preform

at $RR = \frac{4r}{8}$ and $RR = \frac{5r}{8}$. Temperature remains almost constant for a majority of the die stroke and changes only at the end, according to the heat balance. Near the points defined at $RR = \frac{6r}{8}$ and $RR = \frac{7r}{8}$, material flow is confined within the rim cavity and comes in contact under a high pressure at the end of the die stroke. As a result, temperatures at those regions get reduced during that time.

Variation in effective stress has been recorded at the tracking points described earlier (refer to Fig. 13). In case of hot forging, its value depends on both temperature and strain rate. Near the points defined at $RR = \frac{r}{8}$ and $RR = \frac{2r}{8}$, the stress value decreases slowly with stroke showing the predominance of temperature effect. Near the point defined at $RR = \frac{3r}{8}$, the effective stress remains more or less constant due to a balance between the two influencing effects. At the end of forging, material near the points defined at $RR = \frac{4r}{8}$ and $RR = \frac{5r}{8}$ flows through the restricted passage for web region with a high strain rate. The temperature also increases due to excessive friction at the interfaces. The effect of strain rate outperforms the effect of temperature rise, and the effective stress shoots up. Near the points defined at $RR = \frac{6r}{8}$ and $RR = \frac{7r}{8}$, the effect of

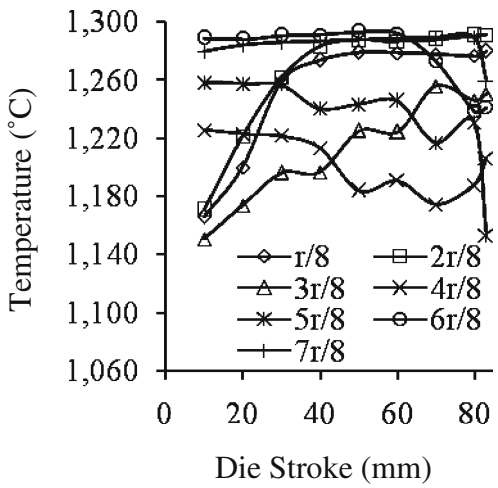

Fig. 12 Temperature at different radius ratios inside the 485 kg blank during forging from 125 mm thick preform

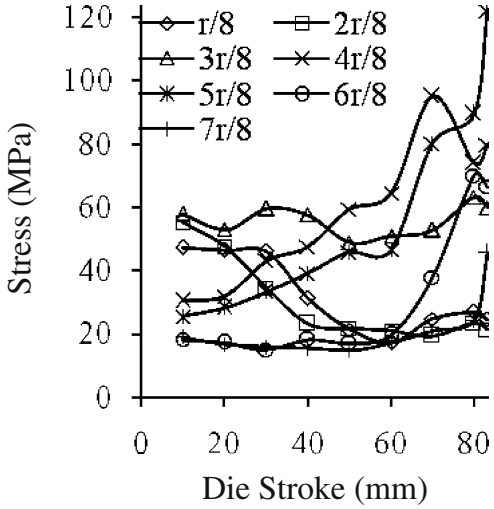

Fig. 13 Magnitude of effective stress at different radius ratios inside the 485 kg blank during forging from 125 mm thick preform

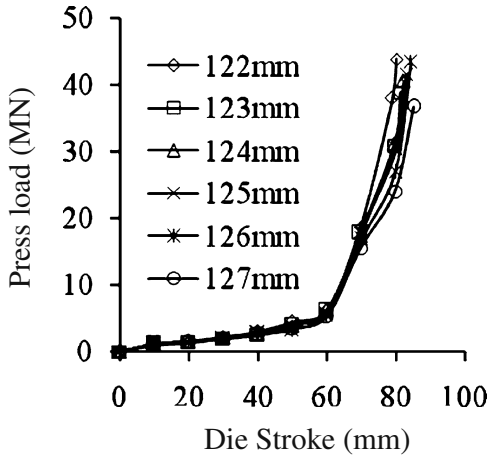

Fig. 15 Forging load for 485 kg blank from preforms of different thickness

temperature on flow stress is found to be high and its value shows some increase at the end of the die stroke. Figure 14 shows the variations of axial stress of the forged wheel during deformation. Up to 60 mm of die stroke, it remains almost the same at all seven tracking points and rises near the completion of the wheel forging. Simulations have been carried out for six preform of same shape but of different heights ranging from 122 to 127 mm and the results (refer to Fig. 15) are analyzed. The maximum temperatures of upper and lower dies at the end of forging have reached to 764°C and 826°C, respectively. The effects of increasing the machining envelop to solve the problems associated with eccentricity; die mismatch and under-filling of die cavity, etc. have also been studied. The FE analysis of $\frac{1}{12}$th model shows an increase in forging load with the increase in blank diameter (refer to Fig. 16).

Closure of folding defect by modifying the die geometry is an important issue. Clear understanding of the propagation of defect is necessary before carrying out any modification. FE simulation has captured the defect propagation and may provide great help in this direction. The location of neutral region has been found in the middle of wheel web, which is an indication of simultaneous filling of the hub and rim cavities of the forging dies [2]. This ensures minimum press load for forging, which is always a requirement in industry. Simulation has predicted the evolution of temperature and variation of effective stress within the forged wheel reasonably well. Axial stress has been found as minimum at the flash gap and increases towards the central part and reaches the maximum value near the axis. This has close similarity with the pattern of axial stress for disk-shaped component [17]. The predicted load for forging $\frac{1}{12}$th of a wheel from 125 mm thick preform is found to be 41.6MN, which is quite reasonable for the material used in this study. The press

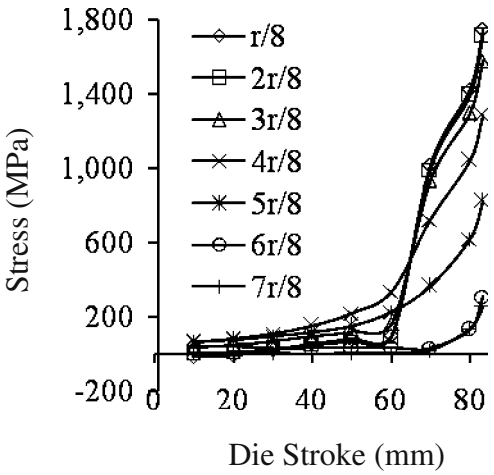

Fig. 14 Axial compressive stress at different radius ratios for 485 kg blank during forging from 125-mm thick preform

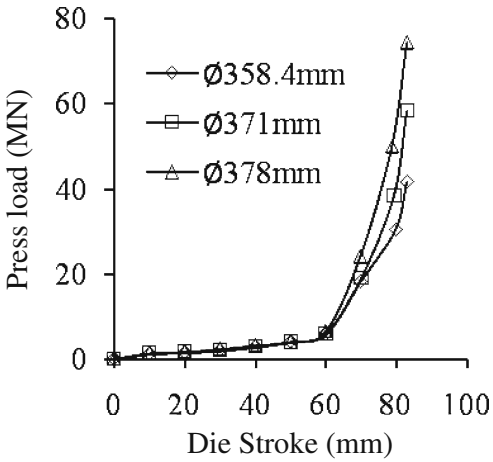

Fig. 16 Forging load for wheels made form blanks of different size using 125-mm thick preform

load is much higher in the forging operation than that in the upsetting operation. It gives an indication that more effort has to be put in optimizing the forging stage. FE results also corroborate that material stiffness increases due to excessive chilling at the flash region. Press load increases rapidly, when the material reaches the flash gap. Design of preform plays a major role in the simultaneous filling of hub and rim cavity, thereby reducing the peak press load. Result of the analysis carried out by slightly varying the preform height has shown that the die cavity gets filled almost simultaneously and there are no significant changes in the press load. This indicates that the used preform geometry is an optimal one The maximum temperatures of upper and lower forging dies are in general agreement to the published results [2]. Simulation has shown that use of additional material increases the press load considerably. Predicted die temperatures at the end of simulation may further be used for calculating the cooling requirement. Die failure occurs, if the effective stress in any part of die exceeds the yield strength at corresponding temperature. Simulated load data may be transferred to calculate die stress considering dies as elastic body, which may further be used in industry for die design and die life estimation.

4.3 Punching of wheel bore

Simulations have been carried out considering the conditions that transfer to punching lower die takes place in 15 s and chilling is done for 7 s using the mesh and thermo-mechanical parameter distribution of forging operation. The maximum and minimum temperatures before punching operation have been recorded as 1266°C and 859°C, respectively.

Number of elements generated for lower die and punch are 22,824 and 6,644, respectively. Critical value of damage factor has been used as 0.89 [2]. FE mesh near the end of punching has been shown in Fig. 17. Seven points have been defined along the punch displacement line (refer to Fig. 18) to collect simulation data.

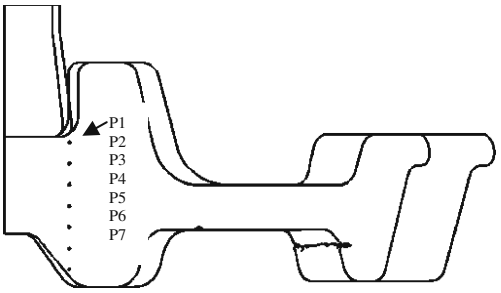

Fig. 18 Seven points separated by 20 mm along the punch movement line have been defined to compare various attributes during punching operation

The temperatures at P1 and P2 are initially dominated by the interface heat loss between the punch and workpiece (refer to Fig. 19). Afterwards, the temperatures at those points increase due to heat generation inside the blank. The points: P3 and P4 are located at the core of the workpiece, which loose heat steadily. At points: P5, P6, and P7, heat generation due to plastic work is seen to be more prominent, and there is a rise in temperature. The maximum and minimum temperatures at the end of punching operation are recorded as 1,252°C and 556°C, respectively. A press load of 0.248MN has been predicted through simulation for punching $\frac{1}{12}$th of the wheel. From Eq. 12, it is clear that in the absence of tensile stress (σ^*) fracture does not occur. The plots of obtained values of axial stress (refer to Fig. 20) also show the presence of tensile stress at points along the punched hole surface. Damage factor as defined in Eq. 12 of an element increases as the material deforms. Once it reaches the critical value, effective stress of the material gets highly reduced. The pattern of changes

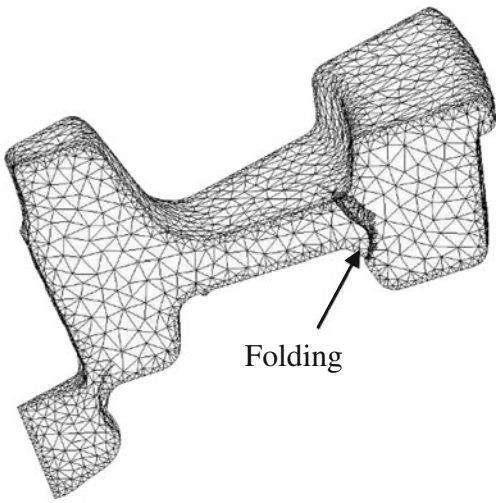

Fig. 17 FE mesh of 485 kg blank during punching of central hole

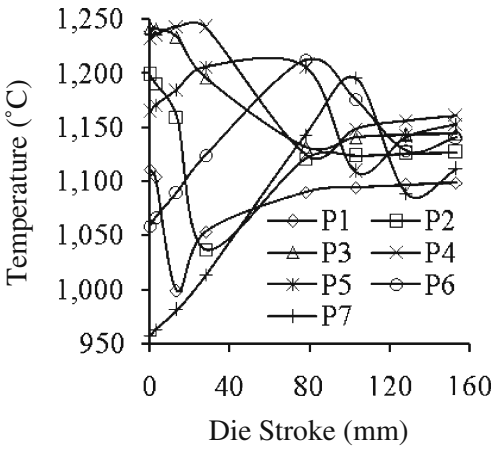

Fig. 19 Temperature at seven different points inside the 485 kg blank during punching of central hole

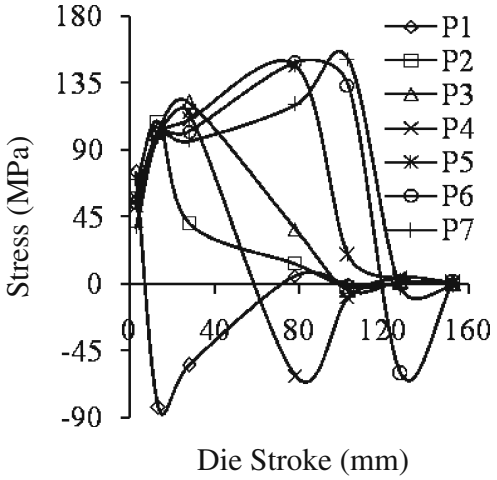

Fig. 20 Axial stress at seven different points inside the 485 kg blank during piercing of central hole

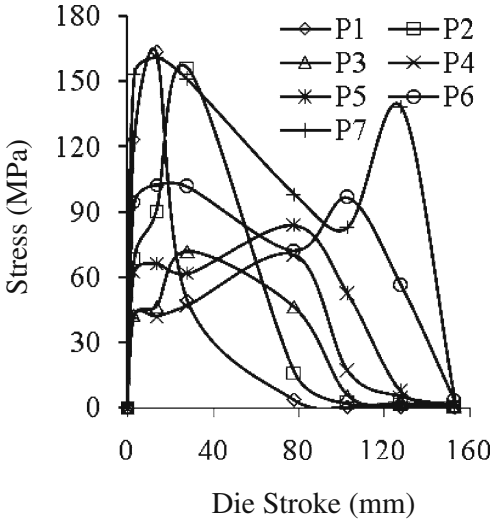

Fig. 22 Effective Stress at seven different points inside the 485 kg blank during punching of central hole

of these two parameters have been studied thoroughly (refer to Figs. 21 and 22). The values of damage factor at points: P1, P2, and P3 increase with die stroke steadily and reach their critical values. As a result, the effective stresses at those points decrease rapidly to very low values. Figure 22 shows that the material for the first two points softens at about 80 mm punch stroke, while that for the third point softens near 100 mm punch stroke. The damage factors for P4, P5, and P6 never attain the value of 0.89. Only, that for point P7 reaches the value of 0.89 at the end of the punch stroke.

Industry requires a burrs-free wheel piercing. Simulation results show that with the used punch radius and clearance, no burrs have been formed. To explain the softening of material at low values of damage factor (refer Eq. 13), the value of mean stress or hydrostatic stress in that zone has been observed. It has been found in FE simulation that a compressive mean stress prevails near the points P4–P6 up to 80 mm of punch stroke, and for rest of the stroke, the mean stress becomes tensile in nature (refer to Table 1). The presence of this compressive mean stress may be the reason behind the low value of damage factor at P4–P6 up to 80 mm of punch stroke and moderate value for punch stroke beyond that. The dominance of tensile mean stress may be the cause of this sharp increase in damage value at P7 at the end of punch stroke.

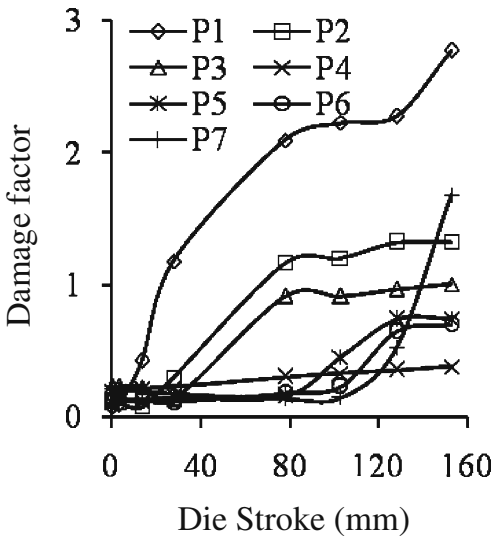

Fig. 21 Value of damage factor at seven different points inside the 485 kg blank during punching of central hole

5 Conclusions

Railway wheel manufacturing process consists of many hot forming and heat transfer stages. Occurrence of errors like, lap formation, under-filling, etc., during one of these stages cannot be identified before the wheels cool down. Reasons for the errors may either be improper optimization of the design of multi-stage process or deviation of the manufacturing process at some stage from the actual design. Reasons for the said deviations are: tapered saw cut in blank, eccentric placement of blank in dies, misalignment of upper and lower dies, improper heating/cooling of dies, excessive heat transfer from workpiece, etc. The work described in this paper involves 3D FE modeling of upsetting, forging, and punching operations including the associated heat transfer stages. The flow of material inside

Table 1 Values of mean stress at the region containing P4, P5, P6, and P7

Stroke (mm)	3	13.5	28	78	103	128	153
Stress (MPa)	−22	−93	−63	−49	21	30	24

the closed die cavity, evolution of various thermo-mechanical properties, and forming loads of the modeled processes have been presented. Punching operation has been modeled in 3D. Variation of cumulative damage factor within the workpiece and the effect of hydrostatic pressure on it have been analyzed. Results have been compared with those of published literature. Simulations have helped to understand the multi-stage process and effects of various thermo-mechanical process parameters on the forged wheel. From the above study, conclusions have been made as follows:

- FE analysis has become matured enough for simulating all processes of multi-stage wheel forging in 3D including furnace heating for the process and tool optimization.
- Formation and propagation of defects through different stages of wheel manufacturing can be observed in 3D.
- Evolution of thermo-mechanical parameters in wheels can be understood thoroughly.
- Process perturbations like eccentricity, die mismatch, and error in blank preparation, etc., can be analyzed in 3D without affecting the regular production. Enhanced knowledge will help in reducing wheel rejection.
- During punching of wheel bore, ductile fracture occurs at a comparatively lower damage value than the supplied damage criterion in presence of compressive mean stress.
- 3D mesh of pierced wheel may be used as input to the subsequent processes simulation.
- Analysis using flow stress data of wheel material nearest to the composition of material available in software library gives details of strain, strain rate, and temperature distribution inside the wheel at different forming stages. This information may be used effectively for planning the testing of actual wheel material to generate the flow stress data.
- Animations of validated results of previously carried out 3D FE analysis can be used by the designers to explain various aspects of wheel forming to the operators in shop-floor in case of a change in product and to give them a prior information of the new wheel in 3D before actual production.

6 Scope of future work

There is no doubt that 3D FE simulation will draw attention of the shop-floor people. However, the problem of high runtime and requirement of validation of the results will restrict its usefulness in wheel production. An alternative way of implementing the advantages of FE analysis in shop-floor is through the use of soft computing-based expert systems (ESs). Once trained, the ESs can produce results in real-time (almost instantaneously), which even the shop-floor people can use for effective decision-making. The authors are working on this problem.

In the area of FE simulation, ring rolling process can be simulated in 3D using the mesh of punched wheel. Process perturbations like eccentricity, die mismatch, etc., can be simulated in 3D, and their effects on rolled wheel can be analyzed. Optimization of the complete multi-stage wheel manufacturing process may be carried out in 3D.

References

1. Santra S (2009) To study the improvement of wheel yield by minimization of rejection due to over-heating during rim spraying and its effect on mechanical properties of railway broad-gauge wheel-steels produced at Durgapur Steel Plant, *M Tech. thesis*, NIT Durgapur, India
2. Ward MJ, Miller BC, Davey K (1998) Simulation of a multi-stage railway wheel and tyre forming process. J Mater Process Technol 80–81:206–212
3. Kim H, Kim J, Kim N (1994) Physical and numerical modeling of hot closed-die forging to reduce forging load and die wear. J Mater Process Technol 42:401–420
4. António CC, Castro CF, Sousa LC (2004) Optimization of metal forming processes. Comput Struct 82:1425–1433
5. Lv C, Zhang L, Mu Z, Tai Q, Zheng Q (2008) 3D FEM simulation of the multi-stage forging process of a gas turbine compressor blade. J Mater Process Technol 198:463–470
6. Davey K, Miller BC, Ward MJ (2001) Efficient strategies for the simulation of railway wheel forming. J Mater Process Technol 118:389–396
7. Santos CA, Aguilar MTP, Campos HB, Pertence AEM, Cetlin PR (2006) Failure analysis of the die in the third hot forging stage of a gear blank. Eng Fail Anal 13:886–897
8. Biba N, Stebounov S, Lishiny A (2001) Cost effective implementation of forging simulation. J Mater Process Technol 113:34–39
9. Hu ZM, Brooks JW, Dean TA (1999) Three-dimensional finite element modeling of forging of a titanium alloy aerofoil sectioned blade. J Manuf Sci Eng 121:366–371
10. Wang-peng D (2008) C Jun, 3D FEA simulation of 4A11 piston skirt isothermal forging process. Trans Nonferrous Met Soc China 18:1196–1200
11. Cockcroft MG, Latham DJ (1968) Ductility and the workability of metals. J Inst Met 96:33–39
12. Ko D-C, Kim D-H, Kim B-M (2002) Finite element analysis for the wear of Ti-N coated punch in the piercing process. Wear 252:859–869
13. Cetinkaya K (2007) A study of the microscopic deformation behavior of a phosphor bronze plate during arbitrary holes piercing process. Mater Des 28:294–300
14. Hartley P, Pillinger I (2006) Numerical simulation of the forging processes. Comput Meth Appl Mech Eng 195:6676–6690
15. Kobayashi S, Oh S-I, Altan T (1989) Metal forming and the finite element method. Oxford University Press, New York
16. Zhang Y, Shan D, Xu F (2009) Flow lines control of disk structure with complex shape in isothermal precision forging. J Mater Process Technol 209:745–753
17. Fereshteh-Sanieee F, Jaafari M (2002) Analytical, numerical and experimental analyses of the closed-die forging. J Mater Process Technol 125–126:334–340
18. Lin YC, Chen M, Zhong J (2008) Prediction of 42CrMo steel flow stress at high temperature and strain rate. Mech Res Commun 35:142–150